JACS Au
AN OPEN ACCESS JOURNAL OF THE AMERICAN CHEMICAL SOCIETY

Open Access
This article is licensed under CC-BY-NC-ND 4.0

pubs.acs.org/jacsau
Perspective

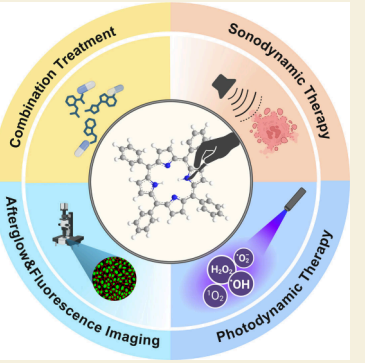
Activatable Porphyrin-Based Sensors, Photosensitizers and Combination Therapeutics

Suritra Bandyopadhyay,[‡] Joseph A Forzano,[‡] Musa Dirak,[‡] and Jefferson Chan*

Cite This: *JACS Au* 2025, 5, 42−54

Read Online
ACCESS | Metrics & More | Article Recommendations

ABSTRACT: Porphyrins, known as the "pigments of life", have evolved from their natural roles into versatile tools for biomedical applications. The development of activatable porphyrins has significantly expanded their utility, enabling precise responses to a carefully selected target analyte. These advances have broadened their use in imaging, diagnosis, and therapy. These capabilities are driven by activity-based sensing (ABS), which enhances the selectivity and sensitivity to various disease biomarkers. However, their design and implementation are intrinsically complex. This perspective provides an easy-to-follow roadmap that details how such molecules can be developed. Furthermore, we highlight recent progress in ABS-modified porphyrins, focusing on how specific modifications achieve these remarkable properties across various biomedical platforms. The ongoing evolution of activatable porphyrins holds great promise for the development of sophisticated, responsive systems, offering more effective diagnostic and therapeutic tools.



KEYWORDS: *porphyrins, biomedical applications, diagnostic tools, therapeutic tools, activity-based sensing*

Downloaded via KOC UNIV on September 3, 2025 at 06:33:09 (UTC).
See https://pubs.acs.org/sharingguidelines for options on how to legitimately share published articles.

1. INTRODUCTION

Since the discovery in 1841, porphyrins such as heme and chlorophyll have been aptly termed the "pigments of life" owing to their pivotal roles in oxygen transport and photosynthesis, respectively.[1,2] However, it was not until 1935, when German chemists Hans Fischer and Wilhelm Gleim prepared the first synthetic porphyrin, that the scientific community gained broader access to these extraordinary compounds.[3] This breakthrough in synthetic chemistry opened new avenues for exploring and manipulating porphyrins, leading to the establishment of reliable structure−function relationships that enabled the modification of the porphyrin scaffold to achieve unique and diverse properties.[4−10] With these advancements, porphyrins have found utility across a range of applications, including biocatalysis, photovoltaic cells, light-emitting materials, and nonlinear optical materials.[11−20] Traditionally, these porphyrins were designed for structural stability to ensure consistent properties. Any alterations during use were often viewed as undesirable due to their potential to complicate signal interpretation. For instance, changes in the aqueous solubility of a porphyrin could affect its effective concentration and thereby impact quantification accuracy. However, recent developments have resulted in a paradigm shift, leading to the intentional design of "activatable" molecules, where structural changes have become engineered features.[21−25] This innovation has significantly expanded the utility of porphyrins, allowing them to switch states in response to a carefully selected target. Activatable porphyrins now play crucial roles in the biomedical field, enabling the imaging, diagnosis, and therapy of various human diseases (e.g., cancer) by responding to specific disease biomarkers.

Porphyrins are inherently complex molecules capable of interacting with a diverse range of stimuli to yield multiple readouts.[26,27] For instance, upon light irradiation in the 400−450 nm (Soret bands) or 500−700 nm (Q bands) wavelength ranges, a porphyrin can become excited, leading to the population of the lowest excited state (S1). This is followed by rapid relaxation to the ground state (S0), emitting fluorescence or releasing heat through radiative and nonradiative pathways, respectively. Due to a large Stokes shift, emission occurs in the deep red region, making porphyrins effective imaging agents for the optical detection of disease biomarkers or as fluorescence-guided surgical tools. Along these lines, porphyrins can serve as photothermal therapy (PTT) agents due to their ability to generate local increases in the temperature. After irradiation, the excited-state porphyrin can relax to the ground state nonradiatively, releasing heat into the local environment and thereby inducing hyperthermia that leads to apoptosis through protein denaturation and membrane disruption. Moreover, excited porphyrins can transition to the first triplet excited state (T1) via intersystem crossing

Received: November 19, 2024
Revised: December 17, 2024
Accepted: December 18, 2024
Published: January 15, 2025



ACS Publications
© 2025 The Authors. Published by American Chemical Society

https://doi.org/10.1021/jacsau.4c01108
JACS Au 2025, 5, 42−54

(ISC), and these triplet excited states can lead to formation of reactive oxygen species (ROS) via electron transfer or via energy transfer that generates toxic singlet oxygen ($^1O_2$) from molecular oxygen ($^3O_2$). This process of ISC and subsequent ROS generation is applied to photodynamic therapy (PDT). The use of ultrasound waves as a stimulus can also trigger the generation of ROS from porphyrins in deeper tissues through an emerging treatment modality known as sonodynamic therapy (SDT). Beyond their interactions with light and sound, porphyrins exhibit a strong propensity to chelate metal ions in the core of the macrocycle, making metal-chelated porphyrins suitable for MRI and PET imaging for whole-body applications.

A promising approach to exploit these various readouts to develop activatable porphyrins is based on a modern design strategy known as activity-based sensing (ABS).[21,23−25] Unlike traditional binding-based detection strategies, such as those utilizing antibodies for labeling, ABS leverages the unique chemical properties and reactivities of the target analyte (Figure 1).[28] This approach is advantageous because it allows

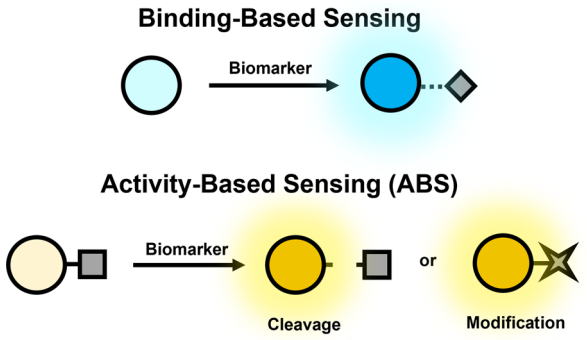


Figure 1. Schematic representation of binding-based sensing vs activity-based sensing molecular platforms and their mechanisms of activation.

for the detection of low-abundance biomarkers through the inclusion of responsive triggers with accelerated reaction rates or those that can undergo signal amplification. Furthermore, when analytes are present in high quantities in healthy tissue, ABS tuning can attenuate the reactivity to prevent false positives. This tunability also enables the design of sensors with exquisite selectivity, capable of distinguishing between similar targets such as one ROS over another.

Given the diverse and complex properties of porphyrins, integrating ABS modifications presents unique challenges compared with many single-modality platforms (e.g., a fluorescent dye developed only for fluorescence imaging). Specifically, maintaining the inherent properties of the porphyrins mentioned above during the incorporation of an ABS trigger requires careful design and optimization. In this Perspective, we provide a roadmap to outline the steps involved in developing such tools. We then summarize recent advances by highlighting activatable ABS porphyrins that have been used in diverse biomedical applications. For brevity, we will not highlight reports employing related structures such as phthalocyanines and chlorins or core-modified expanded/contracted porphyrins.[6,11,29−37] Importantly, we will focus on the ABS design elements, including specific modifications and their impacts on performance. We conclude with a summary of emerging applications in the field and provide our outlook on the continued development of these multifaceted tools across a wide array of applications. We refer readers to other excellent reviews that have covered synthetic strategies, early examples, functional properties, and computational analyses.[1,6,11,35−47]

2. INSTALLING ABS TRIGGERS TO CONTROL PORPHYRIN PROPERTIES

As highlighted in the previous section, porphyrins are inherently complex molecules with the capacity to interact with a diverse range of stimuli to yield multiple readouts. This complexity makes them exceptionally versatile tools in biomedical applications. However, a critical aspect in developing these tools for a desired application lies in the integration of ABS triggers to control the molecule's properties. In this section, we provide a detailed guide on how to effectively install ABS triggers into porphyrins, ensuring their functionality is finely tuned for specific applications (Figure 2).

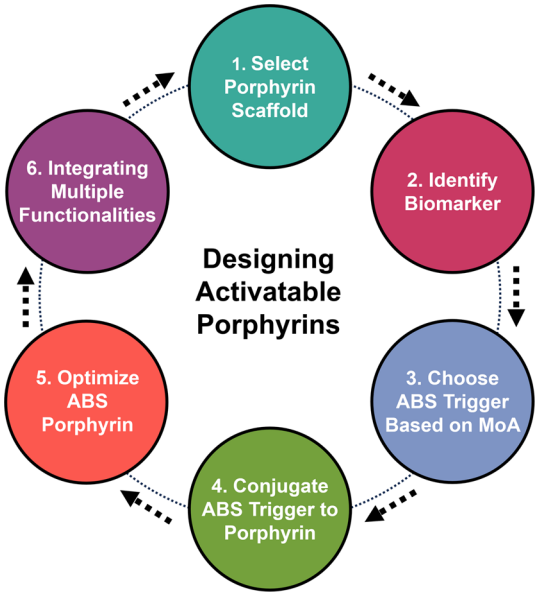


Figure 2. Flowchart to guide how to install ABS triggers effectively into porphyrins.

2.1. Selection of the Appropriate Porphyrin Scaffold

The first step in designing an ABS-modified porphyrin is selecting the appropriate scaffold based on the intended application, whether it is for imaging, therapy, or a combination of both. For instance, if the goal is PDT, a porphyrin with a high $^1O_2$ quantum yield would be an ideal starting point (Figure 3b). For MRI applications, the porphyrin should be coordinated to a paramagnetic metal ion like Gd^{3+} or Mn^{2+}/Mn^{3+} (Figure 3c) to augment signal contrast.[48−53] Key factors to consider include the porphyrin's photophysical and magnetic properties, chemical stability, and biocompatibility.

2.2. Identifying the ABS Trigger

The ABS trigger is a functional group that responds to a specific analyte or disease biomarker. It is crucial to select a trigger that activates only under the desired conditions to avoid off-target effects. Common ABS triggers include enzyme-responsive groups that are cleaved by specific enzymes, pH-sensitive groups that change properties based on (de)-

https://doi.org/10.1021/jacsau.4c01108
JACS Au 2025, 5, 42−54

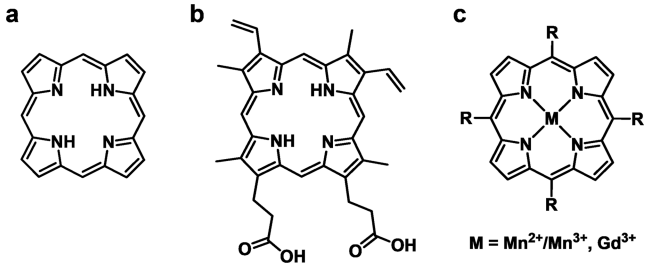


Figure 3. Molecular structure of (a) porphyrin core, (b) protoporphyrin IX (PPIX), an FDA-approved photosensitizer used for PDT, and (c) metalated porphyrin designed for MRI applications, with R groups denoting variable substituents.

protonation, and redox-sensitive groups that respond to changes in oxidative or reductive environments. Additionally, there are a plethora of ABS triggers designed to react selectively to reactive oxygen, nitrogen, and carbonyl species, as well as biological thiols.

2.3. Mechanisms of Activation: Diverting the Excited State and Modulating Magnetic Properties

Once the ABS trigger is installed on the desired porphyrin, it plays a critical role in controlling how the porphyrin responds to an external stimulus. These triggers can modulate its magnetic properties, divert the excited state, or alter its absorption characteristics based on changes to the aggregation state or extent of internal charge transfer. Understanding these mechanisms of activation is key to designing effective ABS-modified porphyrins.

Mechanisms of Activation.

a) Modulation of T1 Relaxation in MRI: ABS triggers can be used to control the T1 relaxation times in MRI by altering the porphyrin's interaction with water molecules, which is crucial for MRI contrast. For instance, a paramagnetic metal ion like Gd^{3+} or Mn^{2+}/Mn^{3+} can be chelated to the selected porphyrin.[31,48−50,52,54,55] The ABS trigger might control the accessibility of water molecules to the metal center. When the trigger is activated, it can either expose or shield the metal center, thereby altering the T1 relaxation time and enhancing or suppressing the MRI contrast.

b) Photoinduced Electron Transfer (PeT): PeT is a common mechanism used in ABS-modified porphyrins whereby an ABS trigger may quench the excited state of the porphyrin. For instance, electron-rich groups like o-phenylenediamine can transfer an electron to the excited porphyrin (acceptor-PeT or a-PeT), preventing fluorescence and other readouts (Figure 4a). Conversely, electron-poor groups such as benzaldehyde or nitrobenzene can accept an electron from the excited porphyrin t
o similarly intercept relaxation pathways (donor-PeT or d-PeT, Figure 4b). However, upon encountering the target analyte (e.g., an enzyme that cleaves the trigger), the PeT is blocked to subsequently allow the porphyrin to fluoresce or generate ROS after ISC.

c) Förster Resonance Energy Transfer (FRET): In some systems, ABS triggers can modulate FRET between the porphyrin and a nearby fluorophore or quencher. When the trigger is intact, energy from the porphyrin's excited state is transferred to the quencher, suppressing fluorescence or ISC. Activation of the trigger disrupts FRET by physically separating the porphyrin from the quencher (via cleavage, See Figure 1) or by changing the energies of molecular orbitals (via chemically modifying the structure, See Figure 1), allowing the porphyrin to emit light or photosensitize.

d) Absorbance Wavelength Shift: An ABS trigger can also induce a shift in the porphyrin's absorbance profile. This can occur if after activation the porphyrin self-assembles to form H- or J-aggregates or the electronic conjugation in the porphyrin core is modified. Likewise, the extent of internal charge transfer can be altered resulting in a shift in the λ_{abs}. These mechanisms allow for selective excitation of the porphyrin at a wavelength that did not previously exhibit a significant absorption before activation.

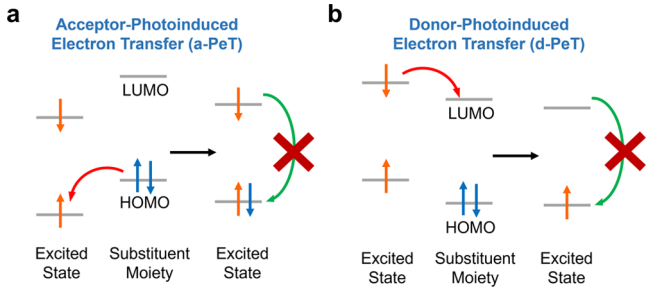


Figure 4. Diagrammatic illustration of a) a-PeT and b) d-PeT quenching.

2.4. Conjugation of the ABS Trigger to the Porphyrin

After identification of the appropriate ABS trigger and understanding its mechanism of activation, the next step is to append it to the porphyrin scaffold. The method of attachment depends on the functional groups present on both the porphyrin and the ABS trigger. Common methods to achieve this include alkylation, carbonate, or carbamate formation, esterification, and amidation, among others. These linkages should be stable under normal conditions unless they are specifically designed to be cleaved by the target analyte.[56−60]

2.5. Optimization of the ABS-Modified Porphyrin

Once the ABS-modified porphyrin is synthesized, rigorous characterization must be performed to ensure it functions as intended. This may involve replacing an ABS trigger with an alternative one targeting the same analyte or modifying the structure of the porphyrin itself if the original does not perform as expected. Next, it is critical to test its responsiveness to the target analyte and verify that the desired readout is produced. Evaluation typically begins with *in vitro* assays where the porphyrin's performance can be evaluated in cell-free systems to establish baseline behavior. After, the ABS-modified porphyrin can be tested in relevant cell lines to evaluate its responsiveness and toxicity in a biological context. Confirmation of target engagement may involve small-molecule inhibition or knockout experiments if the target is an enzyme. Similarly, for ROS or other similar molecules such as NO, treatments that change their cellular levels (either increase or decrease) will serve as important validation tests. Finally, animal studies can be performed to determine the efficacy and safety of porphyrins in living organisms.

https://doi.org/10.1021/jacsau.4c01108
JACS Au 2025, 5, 42−54

2.6. Integrating Multiple ABS Triggers

In some advanced applications, it is beneficial to incorporate multiple ABS triggers within a single porphyrin, creating a logic-gated system that enhances specificity by responding to complex environmental cues (see section 7). In addition, this approach could also be applied to integrate PDT with other combination therapies, drug delivery systems, imaging agents of other modalities, or nanomaterials. When designing such systems, it is important to ensure trigger compatibility so that they do not interfere with each other's function. Additionally, sequential activation may be necessary, where one trigger activates before the other. Finally, incorporating mechanisms for signal amplification can help ensure that the response is strong enough to produce a detectable output, even at low biomarker levels.

3. ACTIVATABLE PORPHYRINS FOR BIOLOGICAL SENSING

Building on the design principles outlined in the previous section, activatable porphyrins can be equipped with ABS triggers that respond to specific enzymes, biologically relevant analytes, and pH changes. However, a key consideration in utilizing porphyrins for these purposes is poor aqueous solubility due to the large hydrophobic tetrapyrrole aromatic core. The solubility of porphyrins can be improved through chemical modifications or by the use of delivery agents. On the other hand, this challenge can also be leveraged as an advantage for ABS designs. By carefully selecting and integrating ABS triggers, researchers can harness the insolubility to enhance the sensitivity and specificity of porphyrin-based sensors. The following studies demonstrate how these principles are applied in the context of biological sensing.

3.1. Enzyme-Responsive Porphyrins

One notable example is the work by Jasanoff and co-workers, who developed Mn-TPPP4 to monitor the activity of secreted alkaline phosphatase (SEAP) in brain tissues.[61] In their study, they designed a water-soluble manganese porphyrin with meso-substituted phosphate-functionalized phenyl groups. Upon cleavage by SEAP in brain tissues, the phosphate groups are removed from the manganese porphyrin, forming a tetrahydroxyphenyl porphyrin that is poorly soluble in aqueous media (Figure 5a–b). Consequently, there is a localized precipitation of the manganese porphyrin, which leads to an observable increase in the T1-weighted MRI signal (Figure 5c–d).

Building on this approach of enzyme-induced precipitation, Haedicke and co-workers reported a similar method to alter MRI properties of their porphyrin.[62] Specifically, they employed a common prodrug approach to improve cellular uptake by altering the polarity of MnIII-tetra(carboxyporphyrin) (MnTCP) by converting polar carboxylate groups to lipophilic acetoxymethyl (AM) esters (MnAMP) (Figure 6a–c). In an aqueous solution, MnAMP exhibits low relaxivity and has a tendency to aggregate. However, upon cleavage by intracellular esterases, the carboxylates are unmasked and MnTCP is retained inside the cell, enhancing the T1 relaxivity through disrupted aggregation.

Expanding the utility of porphyrins to detect various enzymatic activities, researchers also explored the response to heme oxygenase 1 (HO-1), an enzyme linked to atherosclerosis. In this context, Long, Boyle, and co-workers

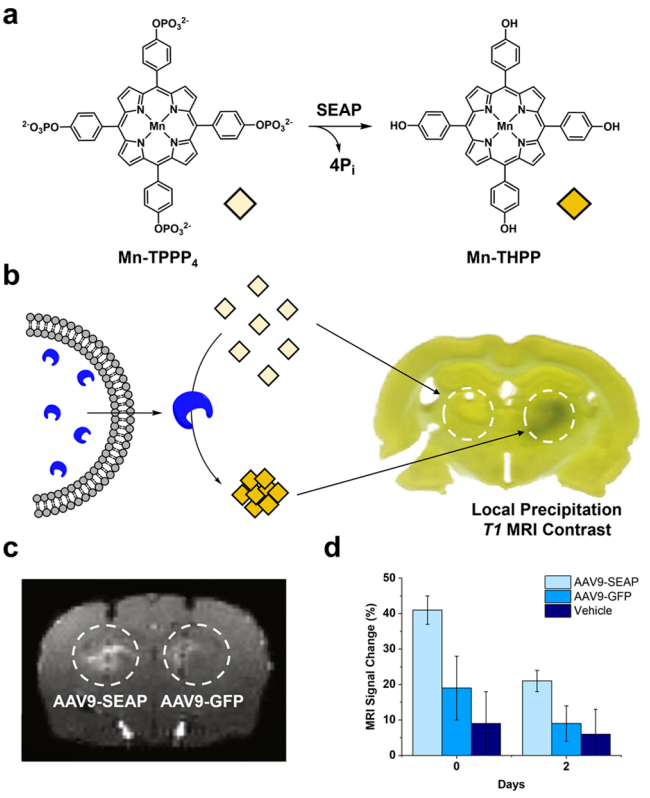


Figure 5. a) Chemical structure and activation of Mn-TPPP$_4$ by SEAP. b) Schematic representation of the local precipitation upon dephosphorylation. c) MRI scans of animals infected with AAV9-SEAP and AAV9-GFP and treated with Mn-TPPP$_4$. d) MRI signal change from AAV9-SEAP, AAV9-GPF and vehicle control groups on days 0 and 2. Adapted from ref 61 with permission from Elsevier, Copyright 2014.

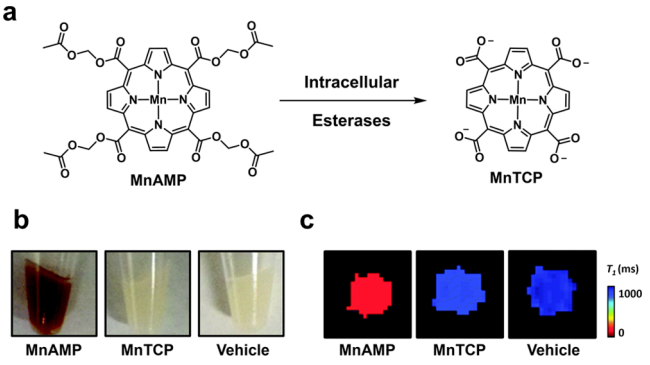


Figure 6. a) Chemical structure and activation of MnAMP with intracellular esterases. b) Photograph of cell pellets treated with MnAMP, MnTCP or vehicle. c) T1 maps of the cell pellets with MnAMP, MnTCP, or vehicle. Adapted from ref 62 with permission from the Royal Society of Chemistry, Copyright 2016.

developed the first chemical probe (Fe-L1) capable of detecting HO-1 activity.[63] Their approach featured a FRET-based design with a symmetric porphyrin Fe-PPIX analogue (dimethyldeuteroheme) connected to a coumarin dye (Figure 7). This platform leveraged the HO-1 catabolic activity of regioselective α-cleavage of Fe-PPIX. As the porphyrin decyclizes, the FRET process is turned off, leading to intensified fluorescence emission of the coumarin scaffold. This design offers intriguing flexibility for the synthesis of more efficient and advanced next-generation probes with more

https://doi.org/10.1021/jacsau.4c01108
JACS Au 2025, 5, 42–54

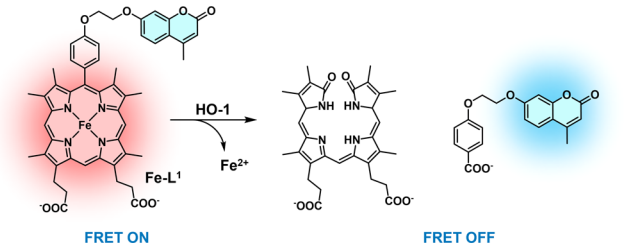


Figure 7. Chemical structure and activation mechanism of Fe-L[1] with the HO-1 enzyme.

favorable near-infrared (NIR) fluorophore pairs, enhancing their utility in cellular and animal models.

Another strategy in the design of activatable porphyrins involves linking a fluorophore to a quencher through molecular beacons - oligonucleotide sequences with stem-loop structures of specific nucleic acid sequences. This concept has been expanded to include peptide sequences that can report the activity of enzymes. Kapoor, Zheng, Chen, and co-workers, for example, strategically designed a matrix metalloproteinase-13 (MMP-13) specific porphyrin molecular beacon ($PP_{MMP13}B$ as is shown in Figure 8a).[64] MMP-13 is a pathological enzyme

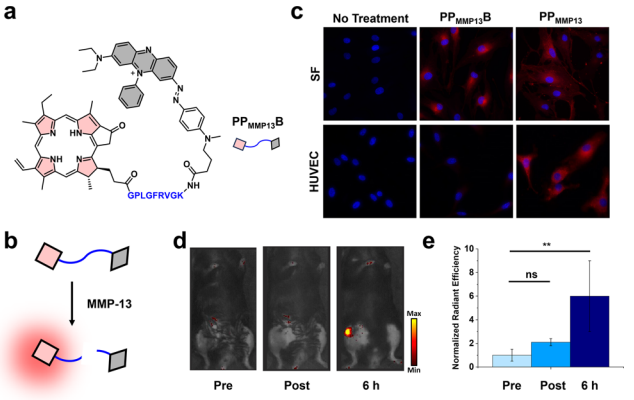


Figure 8. a) Chemical structure of $PP_{MMP13}B$. b) Schematic representation of the peptide cleavage by MMP-13. c) Fluorescence images of SFs and HUVEC cells in the absence or presence of $PP_{MMP13}B$ and PP_{MMP13} (porphyrin fragment with the GPLGFRVGK peptide without the BHQ3 quencher). d) Pre-, post-, and 6 h postinjection images of $PP_{MMP13}B$ in a mouse model of medial meniscus destabilization. e) Quantitative analysis of normalized radiant efficiencies from panel d. Adapted from ref 63 with permission from American Chemical Society, Copyright 2023.

that is known to play a critical role in osteoarthritis. Their platform consisted of a peptide linker substrate for MMP-13 selective cleavage appended to a porphyrin moiety on one end and a quencher on the opposite end to silence the photoactivity of the porphyrin. Upon cleavage by MMP-13, the porphyrin's fluorescence is restored, allowing for MMP-13 expression-dependent fluorescence in patient-derived fibroblast-like synoviocytes and in a murine model of osteoarthritis (Figure 8b–e).

3.2. Environmental Target-Responsive Porphyrins

PeT-based designs have been effectively employed in the development of several environmentally target-responsive porphyrins. In one approach, Okutsu and co-workers developed pH-responsive porphyrins using an a-PeT strategy. Their initial design, N1, featured a single *N,N*-dimethylaniline unit at the meso-position. Upon protonation in acidic environments, this is converted to its anilinium ion, which possesses a lower energy HOMO and thus enables fluorescence emission. They further enhanced the response to pH with N3 and N4 that incorporate three and four aniline units, respectively (Figure 9a). N3, in particular, demonstrated

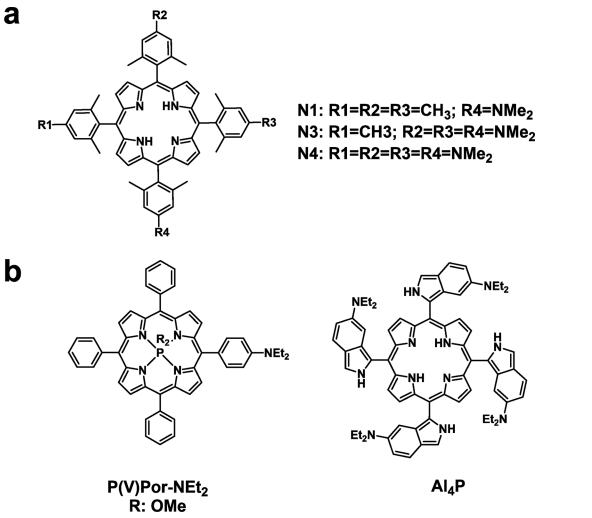


Figure 9. Chemical structure of a) N1–N4, b) P(V)Por-NEt_2, and Al_4P.

a 100-fold increase in the fluorescence turn-on. Subsequent tuning gave rise to water-soluble and red-shifted NIR congeners (Figure 9b).[65−68] In a different application unlike the previous example where a-PeT strategy was used (Figure 10a), Zeng and co-workers employed a donor PeT (d-PeT) mechanism to create a NIR turn-on fluorescence sensor for

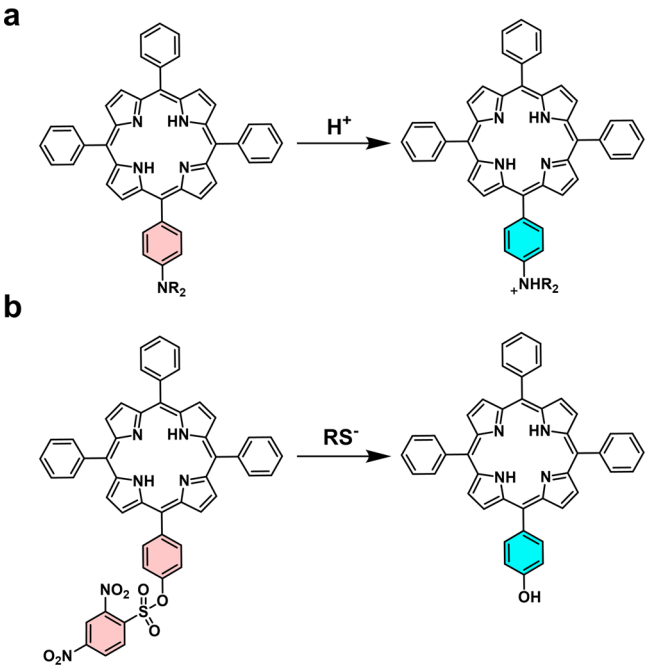


Figure 10. Generalized scheme of a porphyrin with a) an a-PeT substituent moiety and b) a d-PeT substituent moiety. Rings filled with red represent the trigger before reaction with the biomarker, while rings filled with cyan indicate the activated, turned-on product.

https://doi.org/10.1021/jacsau.4c01108
JACS Au 2025, 5, 42−54

sulfide anions (Figure 10b). For d-PeT, the LUMO of the 2,4-dinitrobenzenesulfonyl trigger appended to a para phenol interacts with the excited state of the porphyrin to quench emission. Sulfide-mediated cleavage of this trigger blocks d-PeT to give a fluorescence signal enhancement.[69,70]

4. ACTIVATABLE PORPHYRIN PHOTOSENSITIZERS

Porphyrins have recently been employed as potent photosensitizers and more recently photothermal agents due to their high $^1O_2$ generation capability and photothermal conversion efficiency, respectively. Employing an enzyme-induced precipitation design, Liang and co-workers designed Ac-DEVDD-TPP, a porphyrin that could be readily taken up into cells and cleaved by cysteinyl aspartate-specific proteinase 3 (Caspase 3, Casp3) (Figure 11a–b).[71] In cancer cells overexpressing

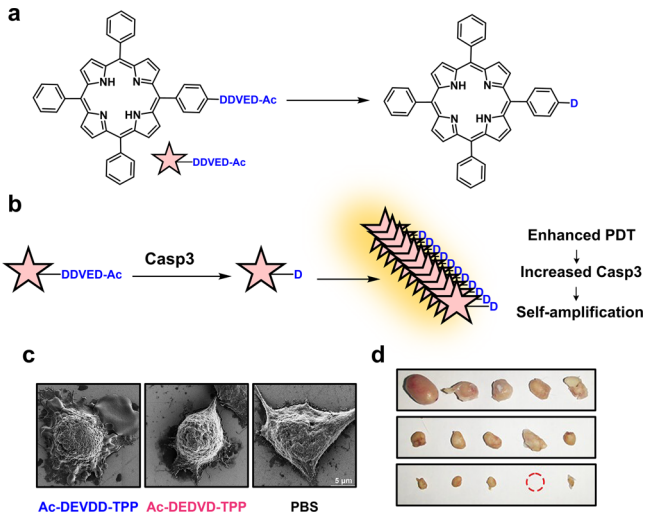


Figure 11. a) Chemical structure of Ac-DEVDD-TPP. b) Schematic illustration of the activation of AC-DEVDD-TPP with Casp3 that leads to self-amplifying PDT. c) SEM images of SCC7 cells pretreated with CDDP, and incubated with Ac-DEVDD-TPP, Ac-DEDVD-TPP, or PBS. d) The tumor photographs at 30 days after excision. First row: treatment with PBS; Second row: treatment with Ac-DEDVD-TPP, CDDP, and light; Third row: treatment with Ac-DEVDD-TPP, CDDP, and light. Adapted from ref 71 with permission from American Chemical Society, Copyright 2023.

Casp3, the resulting product (D-TPP) is substantially more hydrophobic and prone to self-assembly to yield nanofibers. Beyond achieving increased cellular retention, the efficacy of $^1O_2$ generation also improved upon formation of these structures. Moreover, D-TPP fibers enhanced apoptosis (and pyroptosis) and Casp3 expression through PDT in SCC7 cells, making this the first reported "smart" self-amplifying PDT system. Ac-DEVDD-TPP displayed efficient tumor killing in subcutaneous and orthotopic oral murine models of oral squamous cell carcinoma under induced apoptosis when compared to PBS and Ac-DEDVD-TPP, a scrambled peptide control compound not recognized by Casp3 (Figure 11c–d).

Building on the advancements in porphyrin photosensitizers, Zheng and co-workers introduced porphysome NPs for imaging, PTT, and activated PDT in two recent studies (Figure 12a).[72] The original porphysomes consisted of a pyropheophorbide covalently attached to a lipid for self-assembly and cargo encapsulation. Porphysomes exhibit strong absorbance and photoacoustic signals due to self-quenching of

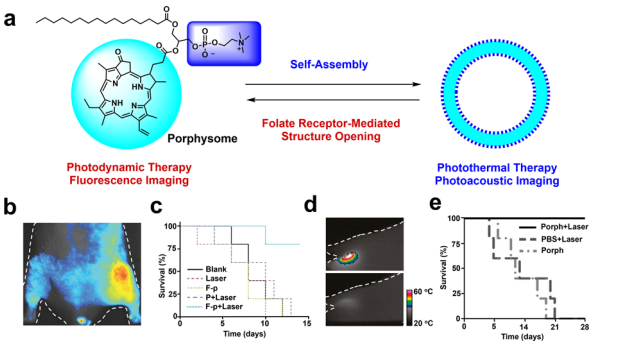


Figure 12. a) Schematic demonstration of self-assembly and folate receptor-mediated structure opening mechanisms of porphysomes. b) Fluorescence images of KB-tumor bearing mouse 24 h after intravenous injection of folate-porphysome. c) Survival rate of KB-tumor bearing mice after treatment with folate porphysome(F-p), nontargeting-porphysome and laser (P+laser), and folate-porphysome plus laser (F-p+laser). d) Thermal images of KB-tumor bearing mouse after intravenous injection of porphysomes (top) or PBS (bottom). e) Survival rate of KB-tumor bearing mice after treatment with PBS plus laser, porphysomes, or porphysomes plus light. Adapted from ref 72 with permission from Springer Nature, Copyright 2011; Adapted from ref 73 with permission from John Wiley & Sons, Inc. Copyright 2014.

adjacent pheophorbide monomers. However, upon uptake into cells, pheophorbide can be liberated by lipases to generate NIR fluorescent signals (Figure 12b). These nanoparticles accumulated in tumors due to their small size (100 nm), where they were used for both photoacoustic imaging and PTT. In a follow-up study, the group took advantage of the disassembly of these structures in cells to liberate the free photosensitizer for activatable PDT. Folate-PEG monomers were included in the porphysome formulation for targeting the folate receptor overexpressed in many cancer cells. While the addition of folate monomers slightly increased the size of the nanoparticles and decreased their circulation time, the porphysomes still exhibited "superquenched" fluorescence and $^1O_2$ production, allowing for selective activation. Upon receptor-mediated endocytosis, the porphysome nanostructure is degraded in the endosome/lysosome to liberate free pyropheophorbide, resulting in vastly increased therapeutic efficacy (Figure 12b–e).[73]

Our lab has recently contributed to this field with the development of NOxPorfin-1, a photosensitizer selectively activated in the presence of nitric oxide (NO) (Figure 13a–c). In this study, we prepared a panel of porphyrins featuring various NO-responsive triggers. Through this work, we discovered that selecting an effective PeT trigger is not as straightforward as it might seem. In particular, typical a-PeT quenchers that would be appropriate for other platforms were largely ineffective, with only the *o*-phenylenediamine trigger successfully suppressing both fluorescence and photosensitization (Figure 13d). Upon interaction with upregulated NO in the microenvironment of solid tumors, NOxPorfin-1 exhibited the highest sensitivity and a robust turn-on response to nanomolar concentrations of NO. This response is mediated by the formation of a triazole ring, which effectively shuts off quenching by the pendant *o*-phenylenediamine. NOxPorfin-1 led to nearly complete ablation of 4T1 breast cancer tumors in BALB/c within just 2 weeks and two rounds of treatment (Figure 13e-f). Importantly, the low steady-state levels of NO in the tumor microenvironment were sufficient to elicit this

https://doi.org/10.1021/jacsau.4c01108
JACS Au 2025, 5, 42–54

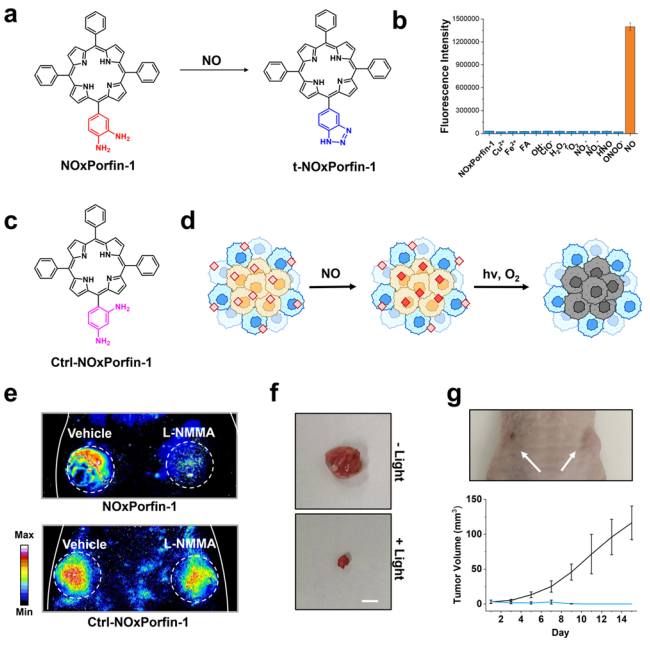


Figure 13. a) Chemical structure and activation of NOxPorfin-1 with NO. b) Selectivity assay of NOxPorfin-1. c) Illustration of NO-selective PDT action of NOxPorfin-1. d) Fluorescence images of mice pretreated with saline (left) or L-NMMA (right) prior to injection of NOxPorfin-1 (top) or Ctrl-NOxPorfin-1 (bottom). e) Photographs of excised tumors after PDT with NOxPorfin-1 on 4T1 murine breast tumor in BALB/c mice. Scale bar: 1 cm. f) Tumor volume curve recorded after administration of NOxPorfin-1 with (blue) or without (black) light treatment on A549 human lung tumors in J/Nu mice. Adapted from ref 74 with permission from American Chemical Society, Copyright 2024.

effect, highlighting the platform's excellent sensitivity to NO (Figure 13g). This approach was further validated in a nascent tumor model, where tumor growth was completely suppressed before tumors could be detected, showing great promise for treating metastatic lesions throughout the body.[74]

While there are many pH activatable porphyrin photosensitizers that are known,[30,75−80] one of particular interest is the pH-activatable transmorphic peptide-based nanomaterial by van Hest and co-workers.[81] These particles are prepared through an amidation reaction between a hydrophobic porphyrin (P) core and a dipeptide consisting of tryptophan and glycine (WG), giving a peptide-porphyrin conjugate (PWG). The fluorescence emission is enhanced owing to the delocalized π-electrons on account of the tryptophan side chain; while glycine introduces carboxyl groups that act as acid-sensitive units. In physiological settings, PWG forms nanoparticles. However, when it reaches the acidic tumor microenvironment, PWG is protonated, thus favoring intermolecular hydrogen bonding with other PWG units, leading to aggregation into nanofibers. The authors employed all-atom molecular dynamics simulations to determine that thermodynamic properties are the driving force for self-assembly. This adaptable nanosystem not only improves tumor retention but also enhances imaging and photodynamic therapeutic efficacy as has been demonstrated by *in vivo* imaging and PDT studies on MCF-7 tumor bearing mice.

Another significant advance in this arena came from the work of Tang and co-workers in developing multimetal metal−organic frameworks (MOFs) that respond specifically to hydrogen sulfide (H_2S) for activated PDT (Figure 14a).[82] Specifically, Zn was coordinated to the tetracarboxyl derivative

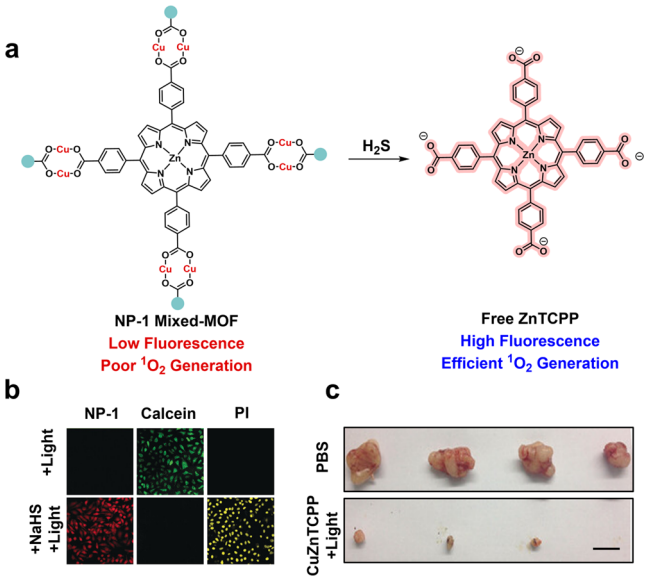


Figure 14. a) Chemical structure and activation of MOF NP-1 with H_2S. b) Confocal images of HepG2 cells stained with PI and calcein AM prior to treatment with NP-1 plus light (top) or NP-1, NaHS and light (bottom). c) Photographs of excised tumors after PDT with NP-1 (bottom) or PBS control (top). Scale bar = 1 cm. Adapted from ref 82. with permission from John Wiley & Sons, Inc. Copyright 2017.

of porphyrin TCPP to generate a potent photosensitizer. By adding Cu^{2+} to these coordinated groups, the fluorescence and photosensitization of the MOFs were significantly quenched. Upon interaction with H_2S, which is upregulated in colon cancer cells, the copper is reduced, and the system showed a dependence on both H_2S and light for effective fluorescence imaging and tumor cell killing (Figure 14b-c). In a similar vein, Zhang and co-workers employed GSH activity to cleave disulfide bonds and release free porphyrin photosensitizer in cancer cells for targeted PDT. They linked the photosensitizer to dendritic oligomers and adamantane, via disulfide bonds, enabling the porphyrins to be uptaken and subsequently released from self-assembled micellar structures for potent activated PDT in cancer cells.[83,84] These disulfide-based monomers also formed nanostructures capable of delivering traditional chemotherapeutics for further anticancer activity.

Lastly, Qu and co-workers developed a biomimetic nanodevice (FKPN) designed for cancer-selective therapy.[85] This nanodevice utilized a neutrophil membrane coating strategy to target tumors and leveraged the GSH abundance in cancer cells to selectively unlock the Fe-porphyrin MOF. The activation proteolytically released the CD95 death domain and caused histone H1 translocation. Additionally, the light-initiated $^1O_2$ generation facilitated DNA double-strand breaks, triggering apoptosis, as the translocated histone H1 bound to CD95 DD, allowing for selective eradication of cancer cells.

5. ACTIVATABLE PORPHYRIN-CONTAINING COMBINATION THERAPEUTICS

PDT represents a viable platform for combination therapy with traditional chemotherapeutics to offer enhanced antitumor efficacy.[75,86−88] An example of this capability is demonstrated in the work by Huang, Zhao, and co-workers, who designed

https://doi.org/10.1021/jacsau.4c01108
JACS Au 2025, 5, 42−54

the nanoagent HA-DQ@MOF for combined chemo- and photo- therapies.[89] In their design, Zn-TCPP (a potent photosensitizer) was coordinated to Cu^{2+} within a host MOF to efficiently quench the fluorescence and PDT activity. A cleavable hyaluronic acid (HA)-diethyldithiocarbamate (DTC) prodrug was also attached to the surface. HA-DQ@MOF selectively targets cancer cells by binding to the CD44 protein on their surface via HA. Once internalized, elevated levels of ROS cleave the HA-DTC prodrug to release free DTC, which is a metabolite of the FDA-approved antialcoholism drug disulfiram with known anticancer effects. However, the specificity of DTC for tumor tissues has been limited. Within the MOF, DTC abstracts Cu^{2+}, generating potent chemotherapeutic $Cu(DTC)_2$ and activating Zn-TCPP photosensitization. This activated photosensitizer generates additional ROS upon laser irradiation, further liberating DTC and amplifying the therapeutic effect. Notably, HA-DQ@MOF remains inert in normal cells with lower ROS levels, increasing selectivity and safety. *In vivo* studies in 4T1 tumor-bearing mice demonstrated significant tumor volume reductions in animals treated with HA-DQ@MOF and light compared with control groups. This work highlights a promising approach for prodrug development and the repurposing of FDA-approved drugs using activatable PDT.

Another notable example of drug delivery is the use of porphyrins as photocleavable protecting groups, where they effectively mask the chemical and biological activity of drugs. Platinum-based antineoplastic drugs, for instance, are commonly used in cancer treatment, but their effectiveness is often hindered by toxic side effects. To address these challenges, Wang and co-workers developed Phorbiplatin, the first small molecule red-light activatable Pt(IV) prodrug (Figure 15).

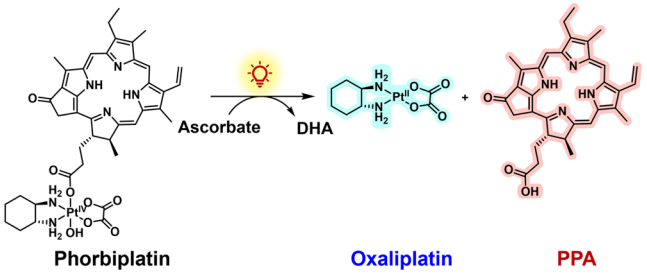


Figure 15. Schematic illustration of the light activation of Phorbiplatin.

Pyropheophorbide A (PPA) was used as the photocage due to its high absorbance in the red region (650 nm) and high $^1O_2$ quantum yield.[90] Upon light irradiation, phosphiniplatin undergoes ISC and transfers energy to ascorbate. This subsequently generates ascorbyl radicals and protons that reduce Pt(IV) to Pt(III). Another reduction event by the ascorbyl radical releases Pt(II) oxaliplatin. Notably, the prodrug exhibits negligible dark toxicity but shows an approximate 1800-fold increase in photocytotoxicity compared to oxaliplatin alone. Mechanistically, PPA and oxaliplatin work together to induce oxidative stress and DNA damage through prodrug activation.

As mentioned previously, beyond photosensitization light can also interact with porphyrins to induce hyperthermia in PTT. Zhang and co-workers explored this dual functionality by designing GNR-ACPI for targeted cancer treatment.[91] GNR-ACPI comprises five components: protoporphyrin IX (PpIX, a known photosensitizer), a cell-penetrating peptide (CPP, polyR chain), a matrix metalloproteinase-2 (MMP-2) sensitive peptide, a blocking peptide (polyE chain), and a gold nanorod (GNR), all linked together. The polyR and polyE peptide chains form strong interactions to keep PpIX and GNR close and blocks photosensitization. In the tumor microenvironment, MMP-2 cleaves the peptides, releasing PpIX-CPP and GNR-polyE. Upon release, PpIX's fluorescence and photosensitization are reactivated for trackable PDT, while the GNR can be used for PTT. The authors demonstrated MMP-2-dependent PDT in various cell lines and observed higher therapeutic efficacy for combined PDT and PTT (depending on the wavelength of irradiation) compared to either treatment alone, both *in cellulo* and *in vivo*.

In a continuation of their work on GSH-responsive porphyrin photosensitizers, Zhang and co-workers developed a combination PDT and chemotherapy approach.[92] By linking the porphyrin photosensitizer to galactose via a disulfide bond, they assembled novel micellar nanosystems capable of encapsulating camptothecin (CPT) in their hydrophobic cores. These systems were designed to target tumor cells through multivalent surface interactions. The micelles themselves (TPP-S-S-Gal) exhibited little dark toxicity in A549 cells, but those containing CPT showed increased dark toxicity, indicating CPT release after disulfide cleavage. Upon irradiation, additional toxicity was observed in CPT-containing micelles compared with TPP-S-S-Gal alone, demonstrating the combination effect of PDT and chemotherapy.

6. EMERGING APPLICATIONS

Despite decades of progress in understanding the intrinsic properties and applications of porphyrins and their derivatives, novel discoveries have continued to be made. Technological advancements now enable deeper exploration of these molecules, leading to significant implications in biology. For instance, Ding and co-workers conducted the first mechanistic investigation into the persistent luminescence behavior of six different commercially available porphyrin derivatives, including PPA, Ce6, HMME, TCPP, TPP, and TAPP.[93] Among these, PPA exhibited the strongest afterglow luminescence following light-mediated $^1O_2$ generation, prompting further exploration into PPA's intrinsic reactivity toward other reactive oxygen and nitrogen species, such as H_2O_2, $O_2^{\bullet-}$, $^{\bullet}OH$, ClO^-, $ONOO^-$, and *t*-Bu-OOH (Figure 16a–b). Their selectivity assays revealed that $ONOO^-$ initiated an intense afterglow luminescence characteristic of PPA. Building on this discovery, PPA was later modified with a self-assembling peptide to form

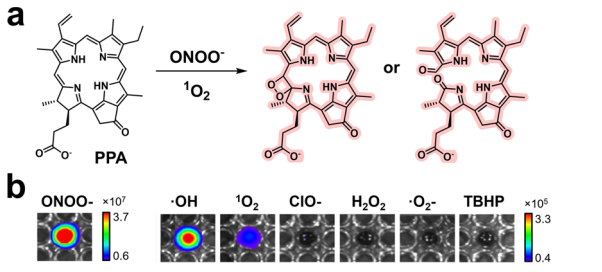


Figure 16. a) Schematic demonstration of the afterglow mechanism of PPA initiated with $ONOO^-$ or $^1O_2$. b) Afterglow images of PPA upon treatment with varying reactive oxygen or nitrogen species. Adapted from ref 93 with permission from John Wiley & Sons, Inc. Copyright 2022.

https://doi.org/10.1021/jacsau.4c01108
JACS Au 2025, 5, 42–54

a tumor-targeting β-sheet structure for *in vivo* $ONOO^-$ detection. This supramolecular nanoassembly was further utilized for tumor monitoring, including scattered tumor nodules, through persistent luminescence and the photoacoustic channel. Additionally, it was employed to screen immunogenic cell death drugs in animal models.

Leveraging afterglow luminescence as an emerging imaging modality, Miao and co-workers reported the utility of porphyrin-based afterglow luminescence sensors for glutathione (GSH) in cancer biology. They coassembled a porphyrin-based luminophore (TPP-DO) with an amphiphilic triblock copolymer to fabricate biocompatible afterglow nanoparticles (NPs) (Figure 17a–c).[94] The TPP-DO structure

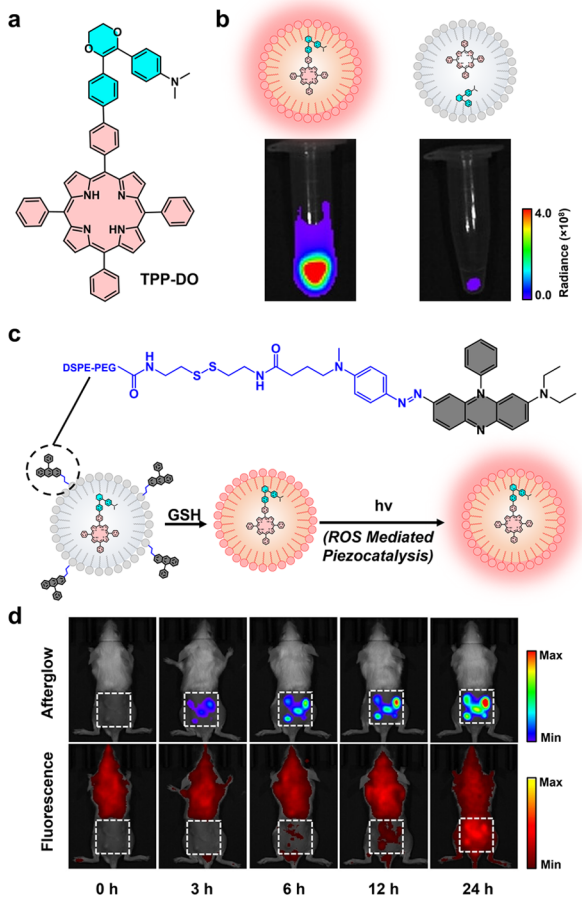


Figure 17. a) Chemical structure of TPP-DO. b) Afterglow images of TPP-DO NPs through intramolecular (left) or intermolecular (right) energy transfer. c) Schematic demonstration of GSH-driven activation. d) Afterglow and fluorescence images of 4T1-tumor bearing mice following the intravenous administration of Q-TPP-DO. Adapted from ref 94 with permission from John Wiley & Sons, Inc. Copyright 2023.

features a meso-tetraphenylporphyrin-based photosensitizer and a singlet oxygen ($^1O_2$) sensitive relay unit that forms a 1,2-dioxetane intermediate upon irradiation. After decomposition, the intermediate produces afterglow luminescence that is visible under chicken tissue of 6 cm thickness. TPP-DO was further converted into a GSH-responsive afterglow handle by using a disulfide-bond-bearing black hole quencher 3 (BHQ3). Upon cleavage by GSH, free TPP-DO is released and can be tracked via afterglow luminescence for *in vivo* real-time tumor monitoring and surgical navigation of microtumors (Figure 17d).

While porphyrins are often used to induce cell death independently, their light-harvesting abilities also offer the potential to create potent photocages capable of releasing toxic payloads only at the site of irradiation.[95−99] In a recent report exploring this potential, Weinstain, Klán, and co-workers developed a modular porphyrin photocleavable protecting group (PPG) design.[100] By leveraging the mesofunctional handles provided by porphyrin scaffolds, multiple leaving groups were incorporated onto the same core, enhancing the release of the cargo of interest. Specifically, they synthesized meso-methylporphyrin-protected indibulin (a tubulin assembly inhibitor) and methotrexate, an antifolate agent, as leaving groups (LGs) for evaluating functionality in a complex cellular environment (Figure 18a). Furthermore, the platform

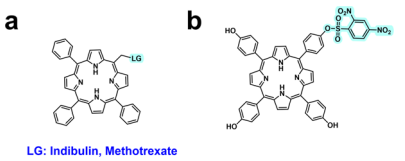


Figure 18. Chemical structures of a) photocleavable porphyrins and b) GSH responsive prodrug sonosensitizer

demonstrated tunable drug-release capabilities via chelation of transition metal complexes, with DMAP serving as the LG. Notably, chelation with Zinc and Palladium resulted in higher photodecomposition quantum yields than the metal-free ligand, whereas copper and nickel did not facilitate photoactivated release. Particularly interesting was the extraordinarily high uncaging cross section observed for the zinc-chelated complex.

Light-initiated therapies are highly effective for treating cancer and other conditions of the skin and at shallow tissue depths. However, they are less effective in deep tissue environments due to the attenuation of both excitation and emission of light by endogenous absorbers. One promising approach to overcoming this limitation involves the use of ultrasonic waves rather than light for excitation as sound can penetrate tissue more effectively. An and co-workers formulated a GSH-responsive tetrahydroxy porphyrin-derived prodrug for cancer-selective SDT (Figure 18b).[101] ROS assays revealed that the probe generated $^1O_2$ and $^{\bullet}OH$ upon ultrasonic irradiation. Due to their hydrophobic nature, prodrug molecules were further encapsulated into DSPE-PEG5000 NPs via membrane hydration to ensure biocompatible imaging and SDT in animal models. Owing to the GSH-facilitated activation, a high tumor-to-normal muscle fluorescence ratio (8.9) was observed in 4T1 tumor-bearing mice 24 h after injection. Ultrasound-induced tumor growth suppression was successfully demonstrated in the prodrug NP-treated tumor-bearing mice.

A key challenge of bringing PDT into the clinic is the decreased efficacy within hypoxic tumor microenvironments, where the interaction with oxygen ($^3O_2$) is required to generate highly reactive $^1O_2$. To address this issue, Xu and co-workers developed a novel pyridinium-substituted porphyrin (TMPyP), which functions as a traditional photosensitizer when irradiated with white light in the presence of oxygen.[102] However, when reduced to phlorin by reductive facultative anaerobes, TMPyP also serves as an effective PTT agent.

https://doi.org/10.1021/jacsau.4c01108
JACS Au 2025, 5, 42−54

Instead of generating ROS, PTT induces hyperthermia, causing cell death by absorbing incident light energy and releasing it as heat. In comparison to TMPyP, phlorin exhibits an NIR absorption band, which was leveraged for selective photothermal activation with the appropriate wavelength of light. Both TMPyP and the phlorin product showed complete inhibition of bacterial colony formation when used as PS and PTT agent, respectively. Interestingly, while TMPyP was effective against nonreducing bacterial strains, phlorin acted on reductive facultative anaerobic strains. Furthermore, caging the positively charged pyridinium rings with cucurbit[7]uril suppressed dark toxicity in mammalian cells without compromising the therapeutic efficacy, as demonstrated in a murine model of bacterial infection. This ability to leverage chemical changes in distinct biological contexts for the application of multiple therapeutic modalities offers a promising strategy to overcome the inefficiencies of PDT in hypoxic environments.

7. CONCLUSION AND OUTLOOK

Activatable porphyrins have emerged as powerful tools in biomedical research, offering excellent specificity in both diagnostics and therapy. However, beyond leveraging a single disease-biomarker for activation, one promising direction is the incorporation of logic-gated designs, where porphyrins could be activated only under specific combinations of stimuli. This will be enabled by the evolution of more sophisticated ABS designs. We envision that this would allow for the creation of porphyrins tailored to serve as multimodal imaging agents, dynamic drug delivery systems, and other advanced tools that can adapt to complex biological environments. Structurally modifying porphyrins to interact with light across different wavelengths (e.g., short-wave infrared) represents another area we anticipate emerging. Indeed, this could lead to applications in deeper tissues and present new opportunities for multiplexing. Furthermore, modifications to the porphyrin core could lead to the development of molecules responsive to a broader range of stimuli including mechanical, electrical, or thermal cues. In terms of readouts, the field is poised to move beyond traditional modalities, such as fluorescence, PET, and MRI. Emerging techniques such as afterglow luminescence, photoacoustic imaging, and sonodynamic therapy are setting the stage for exciting new applications. Integrating these systems with cutting-edge fields such as optogenetics and bioelectronic medicine could revolutionize real-time disease monitoring and treatment. Continued research and development in each of these areas will undoubtedly lead to breakthroughs that can address the most challenging issues in modern healthcare.

AUTHOR INFORMATION

Corresponding Author

Jefferson Chan − *Department of Chemistry, Cancer Center at Illinois and Beckman Institute for Advanced Science and Technology, University of Illinois at Urbana−Champaign, Urbana 61801 Illinois, United States;* orcid.org/0000-0003-4139-4379; Email: jeffchan@illinois.edu

Authors

Suritra Bandyopadhyay − *Department of Chemistry, Cancer Center at Illinois and Beckman Institute for Advanced Science and Technology, University of Illinois at Urbana−Champaign, Urbana 61801 Illinois, United States*

Joseph A Forzano − *Department of Chemistry, Cancer Center at Illinois and Beckman Institute for Advanced Science and Technology, University of Illinois at Urbana−Champaign, Urbana 61801 Illinois, United States;* orcid.org/0000-0002-2839-7797

Musa Dirak − *Department of Chemistry, Cancer Center at Illinois and Beckman Institute for Advanced Science and Technology, University of Illinois at Urbana−Champaign, Urbana 61801 Illinois, United States; Department of Chemistry, Koç University, 34450 Istanbul, Türkiye;* orcid.org/0000-0002-2085-2345

Complete contact information is available at: https://pubs.acs.org/10.1021/jacsau.4c01108

Author Contributions

‡S.B., J.A.F. and M.D. contributed equally.

Notes

The authors declare no competing financial interest.

ACKNOWLEDGMENTS

S.B. is thankful for the support from the Arnold and Mabel Beckman Foundation for his Beckman Graduate Fellowship. M.D. is thankful for support via the International Research Fellowship Programme for PhD Students (TUBITAK 2214-A). TOC artwork created with Biorender.com.

REFERENCES

(1) Senge, M. O.; Sergeeva, N. N.; Hale, K. J. Classic Highlights in Porphyrin and Porphyrinoid Total Synthesis and Biosynthesis. *Chem. Soc. Rev.* **2021**, *50* (7), 4730−4789.

(2) Battersby, A. R. Tetrapyrroles: The Pigments of Life. *Nat. Prod. Rep.* **2000**, *17* (6), 507−526.

(3) Fischer, H.; Gleim, W. Synthese Des Porphins. *Liebigs Ann.* **1936**, *521* (1), 157−160.

(4) Adler, A. D.; Longo, F. R.; Finarelli, J. D.; Goldmacher, J.; Assour, J.; Korsakoff, L. A Simplified Synthesis for Meso-Tetraphenylporphine. *J. Org. Chem.* **1967**, *32* (2), 476−476.

(5) Rothemund, P. A New Porphyrin Synthesis. The Synthesis of Porphin1. *J. Am. Chem. Soc.* **1936**, *58* (4), 625−627.

(6) Tanaka, T.; Osuka, A. Conjugated Porphyrin Arrays: Synthesis, Properties and Applications for Functional Materials. *Chem. Soc. Rev.* **2015**, *44* (4), 943−969.

(7) Zhao, Y.; Hu, Y.; Zhong, Y.; Wang, J.; Liu, Z.; Bai, F.; Zhang, D. Missing Links between the Structures and Optical Properties of Porphyrin Assemblies. *J. Phys. Chem. C* **2021**, *125* (40), 22318−22327.

(8) Misra, R.; Chandrashekar, T. K. Structural Diversity in Expanded Porphyrins. *Acc. Chem. Res.* **2008**, *41* (2), 265−279.

(9) Su, W.; Cooper, T. M.; Tang, N.; Krein, D.; Jiang, H.; Brandelik, D.; Fleitz, P.; Brant, M. C.; Mclean, D. G. Structure-Optical Property Relationships of Porphyrins. *MRS Proceedings* **1997**, *479*, 313−318.

(10) Silva, E. F. F.; Serpa, C.; Dabrowski, J. M.; Monteiro, C. J. P.; Formosinho, S. J.; Stochel, G.; Urbanska, K.; Simoes, S.; Pereira, M. M.; Arnaut, L. G. Mechanisms of Singlet-Oxygen and Superoxide-Ion Generation by Porphyrins and Bacteriochlorins and Their Implications in Photodynamic Therapy. *Chem.—Eur. J.* **2010**, *16* (30), 9273−9286.

(11) Sessler, J. L.; Seidel, D. Synthetic Expanded Porphyrin Chemistry. *Angew. Chem., Int. Ed.* **2003**, *42* (42), 5134−5175.

(12) Barona-Castaño, J.; Carmona-Vargas, C.; Brocksom, T.; de Oliveira, K. Porphyrins as Catalysts in Scalable Organic Reactions. *Molecules* **2016**, *21* (3), 310.

(13) Min Park, J.; Lee, J. H.; Jang, W.-D. Applications of Porphyrins in Emerging Energy Conversion Technologies. *Coord. Chem. Rev.* **2020**, *407*, 213157.
(14) Shi, R.; Han, X.; Xu, J.; Bu, X. Crystalline Porous Materials for Nonlinear Optics. *Small* **2021**, *17* (22), 2006416.
(15) Li, L.-L.; Diau, E. W.-G. Porphyrin-Sensitized Solar Cells. *Chem. Soc. Rev.* **2013**, *42* (1), 291−304.
(16) Kesters, J.; Verstappen, P.; Kelchtermans, M.; Lutsen, L.; Vanderzande, D.; Maes, W. Porphyrin-Based Bulk Heterojunction Organic Photovoltaics: The Rise of the Colors of Life. *Adv. Energy Mater.* **2015**, *5* (13), 1500218.
(17) Mrinalini, M.; Naresh, M.; Prasanthkumar, S.; Giribabu, L. Porphyrin-Based Supramolecular Assemblies and Their Applications in NLO and PDT. *J. Porphyr. Phthalocyanines* **2021**, *25* (05n06), 382−395.
(18) Senge, M. O.; Fazekas, M.; Notaras, E. G. A.; Blau, W. J.; Zawadzka, M.; Locos, O. B.; Ni Mhuircheartaigh, E. M. Nonlinear Optical Properties of Porphyrins. *Adv. Mater.* **2007**, *19* (19), 2737−2774.
(19) Collman, J. P.; Zhang, X.; Lee, V. J.; Uffelman, E. S.; Brauman, J. I. Regioselective and Enantioselective Epoxidation Catalyzed by Metalloporphyrins. *Science* **1993**, *261* (5127), 1404−1411.
(20) Ricoux, R.; Sauriat-Dorizon, H.; Girgenti, E.; Blanchard, D.; Mahy, J.-P. Hemoabzymes: Towards New Biocatalysts for Selective Oxidations. *J. Immunol. Methods* **2002**, *269* (1−2), 39−57.
(21) Bruemmer, K. J.; Crossley, S. W. M.; Chang, C. J. Activity-Based Sensing: A Synthetic Methods Approach for Selective Molecular Imaging and Beyond. *Angew. Chem., Int. Ed.* **2020**, *59* (33), 13734−13762.
(22) Baruch, A.; Jeffery, D. A.; Bogyo, M. Enzyme Activity - It's All about Image. *Trends Cell Biol.* **2004**, *14* (1), 29−35.
(23) Gardner, S. H.; Reinhardt, C. J.; Chan, J. Advances in Activity-Based Sensing Probes for Isoform-Selective Imaging of Enzymatic Activity. *Angew. Chem., Int. Ed.* **2021**, *60* (10), 5000−5009.
(24) Chan, J.; Dodani, S. C.; Chang, C. J. Reaction-Based Small-Molecule Fluorescent Probes for Chemoselective Bioimaging. *Nat. Chem.* **2012**, *4* (12), 973−984.
(25) East, A. K.; Lucero, M. Y.; Chan, J. New Directions of Activity-Based Sensing for in Vivo NIR Imaging. *Chem. Sci.* **2021**, *12* (10), 3393−3405.
(26) Imran, M.; Ramzan, M.; Qureshi, A.; Khan, M.; Tariq, M. Emerging Applications of Porphyrins and Metalloporphyrins in Biomedicine and Diagnostic Magnetic Resonance Imaging. *Biosensors* **2018**, *8* (4), 95.
(27) Tsolekile, N.; Nelana, S.; Oluwafemi, O. S. Porphyrin as Diagnostic and Therapeutic Agent. *Molecules* **2019**, *24* (14), 2669.
(28) Messina, M. S.; Quargnali, G.; Chang, C. J. Activity-Based Sensing for Chemistry-Enabled Biology: Illuminating Principles, Probes, and Prospects for Boronate Reagents for Studying Hydrogen Peroxide. *ACS Bio Med. Chem. Au* **2022**, *2* (6), 548−564.
(29) Mody, T. D.; Sessler, J. L. Porphyrin- and Expanded Porphyrin-Based Diagnostic and Therapeutic Agents. *Supramolecular Materials and Technologies*; John Wiley and Sons, 1999; pp 245−294.
(30) Chen, J.; Sedgwick, A. C.; Sen, S.; Ren, Y.; Sun, Q.; Chau, C.; Arambula, J. F.; Sarma, T.; Song, L.; Sessler, J. L.; Liu, C. Expanded Porphyrins: Functional Photoacoustic Imaging Agents That Operate in the NIR-II Region. *Chem. Sci.* **2021**, *12* (29), 9916−9921.
(31) Ren, Y.; Sedgwick, A. C.; Chen, J.; Thiabaud, G.; Chau, C. V.; An, J.; Arambula, J. F.; He, X.-P.; Kim, J. S.; Sessler, J. L.; Liu, C. Manganese(II) Texaphyrin: A Paramagnetic Photoacoustic Contrast Agent Activated by Near-IR Light. *J. Am. Chem. Soc.* **2020**, *142* (38), 16156−16160.
(32) Zheng, B.-D.; Ye, J.; Zhang, X.-Q.; Zhang, N.; Xiao, M.-T. Recent Advances in Supramolecular Activatable Phthalocyanine-Based Photosensitizers for Anti-Cancer Therapy. *Coord. Chem. Rev.* **2021**, *447*, 214155.
(33) Chandrashekar, T. K.; Venkatraman, S. Core-Modified Expanded Porphyrins: New Generation Organic Materials. *Acc. Chem. Res.* **2003**, *36* (9), 676−691.
(34) Chmielewski, P. J.; Latos-Grazynski, L.ła. Core Modified Porphyrins - a Macrocyclic Platform for Organometallic Chemistry. *Coord. Chem. Rev.* **2005**, *249* (21−22), 2510−2533.
(35) Saito, S.; Osuka, A. Expanded Porphyrins: Intriguing Structures, Electronic Properties, and Reactivities. *Angew. Chem., Int. Ed.* **2011**, *50* (19), 4342−4373.
(36) Tanaka, T.; Osuka, A. Chemistry of Meso-Aryl-Substituted Expanded Porphyrins: Aromaticity and Molecular Twist. *Chem. Rev.* **2017**, *117* (4), 2584−2640.
(37) Sessler, J. L.; Gross, Z.; Furuta, H. Introduction: Expanded, Contracted, and Isomeric Porphyrins. *Chem. Rev.* **2017**, *117* (4), 2201−2202.
(38) Hiroto, S.; Miyake, Y.; Shinokubo, H. Synthesis and Functionalization of Porphyrins through Organometallic Methodologies. *Chem. Rev.* **2017**, *117* (4), 2910−3043.
(39) Lindsey, J. S. Synthetic Routes to Meso-Patterned Porphyrins. *Acc. Chem. Res.* **2010**, *43* (2), 300−311.
(40) Lee, H.; Hong, K.-I.; Jang, W.-D. Design and Applications of Molecular Probes Containing Porphyrin Derivatives. *Coord. Chem. Rev.* **2018**, *354*, 46−73.
(41) Park, J. M.; Hong, K.-I.; Lee, H.; Jang, W.-D. Bioinspired Applications of Porphyrin Derivatives. *Acc. Chem. Res.* **2021**, *54* (9), 2249−2260.
(42) Tian, J.; Huang, B.; Nawaz, M. H.; Zhang, W. Recent Advances of Multi-Dimensional Porphyrin-Based Functional Materials in Photodynamic Therapy. *Coord. Chem. Rev.* **2020**, *420*, 213410−213410.
(43) Shi, Y.; Zhang, F.; Linhardt, R. J. Porphyrin-Based Compounds and Their Applications in Materials and Medicine. *Dyes Pigm.* **2021**, *188*, 109136.
(44) Zhang, X.; Wasson, M. C.; Shayan, M.; Berdichevsky, E. K.; Ricardo-Noordberg, J.; Singh, Z.; Papazyan, E. K.; Castro, A. J.; Marino, P.; Ajoyan, Z.; Chen, Z.; Islamoglu, T.; Howarth, A. J.; Liu, Y.; Majewski, M. B.; Katz, M. J.; Mondloch, J. E.; Farha, O. K. A Historical Perspective on Porphyrin-Based Metal-Organic Frameworks and Their Applications. *Coord. Chem. Rev.* **2021**, *429*, 213615.
(45) Roznyatovskiy, V. V.; Lee, C.; Sessler, J. L. π-Extended Isomeric and Expanded Porphyrins. *Chem. Soc. Rev.* **2013**, *42* (5), 1921−1933.
(46) Cuesta, L.; Sessler, J. L. π-Metal Complexes of Tetrapyrrolic Systems. A Novel Coordination Mode in "Porphyrin-Like" Chemistry. *Chem. Soc. Rev.* **2009**, *38* (9), 2716.
(47) Sessler, J. L.; Tomat, E. Transition-Metal Complexes of Expanded Porphyrins. *Acc. Chem. Res.* **2007**, *40* (5), 371−379.
(48) Vollett, K. D. W.; Szulc, D. A.; Cheng, H.-L. M. A Manganese Porphyrin Platform for the Design and Synthesis of Molecular and Targeted MRI Contrast Agents. *Int. J. Mol. Sci.* **2023**, *24* (11), 9532−9532.
(49) Zang, L.; Zhao, H.; Hua, J.; Qin, F.; Zheng, Y.; Zhang, Z.; Cao, W. Water-Soluble Gadolinium Porphyrin as a Multifunctional Theranostic Agent: Phosphorescence-Based Oxygen Sensing and Photosensitivity. *Dyes Pigm.* **2017**, *142*, 465−471.
(50) Luo, J.; Chen, L.-F.; Hu, P.; Chen, Z.-N. Tetranuclear Gadolinium(III) Porphyrin Complex as a Theranostic Agent for Multimodal Imaging and Photodynamic Therapy. *Inorg. Chem.* **2014**, *53* (8), 4184−4191.
(51) Jahanbin, T.; Sauriat-Dorizon, H.; Spearman, P.; Benderbous, S.; Korri-Youssoufi, H. Development of Gd(III) Porphyrin-Conjugated Chitosan Nanoparticles as Contrast Agents for Magnetic Resonance Imaging. *Mater. Sci. Eng., C* **2015**, *52*, 325−332.
(52) Venter, A.; Szulc, D. A.; Loai, S.; Ganesh, T.; Haedicke, I. E.; Cheng, H.-L. M. A Manganese Porphyrin-Based T1 Contrast Agent for Cellular MR Imaging of Human Embryonic Stem Cells. *Sci. Rep.* **2018**, *8* (1), 12129.
(53) Thiabaud, G. D.; Schwalm, M.; Sen, S.; Barandov, A.; Simon, J.; Harvey, P.; Spanoudaki, V.; Müller, P.; Sessler, J. L.; Jasanoff, A. Texaphyrin-Based Calcium Sensor for Multimodal Imaging. *ACS Sens.* **2023**, *8* (10), 3855−3861.
(54) Zhang, X.; Lovejoy, K. S.; Jasanoff, A.; Lippard, S. J. Water-Soluble Porphyrins as a Dual-Function Molecular Imaging Platform

https://doi.org/10.1021/jacsau.4c01108
JACS Au 2025, 5, 42−54

for MRI and Fluorescence Zinc Sensing. *Proc. Natl. Acad. Sci. U.S.A.* **2007**, *104* (26), 10780−10785.
(55) Lee, T.; Zhang, X.; Dhar, S.; Faas, H.; Lippard, S. J.; Jasanoff, A. In Vivo Imaging with a Cell-Permeable Porphyrin-Based MRI Contrast Agent. *Cell Chem. Biol.* **2010**, *17* (6), 665−673.
(56) Zhang, X.; Xiu, T.; Wang, H.; Wang, H.; Li, P.; Tang, B. Recent Progress in the Development of Small-Molecule Double-Locked Logic Gate Fluorescence Probes. *Chem. Commun.* **2023**, *59* (74), 11017−11027.
(57) Chen, M.; Wang, C.; Ding, Z.; Wang, H.; Wang, Y.; Liu, Z. A Molecular Logic Gate for Developing "AND" Logic Probes and the Application in Hepatopathy Differentiation. *ACS Cent. Sci.* **2022**, *8* (6), 837−844.
(58) Wu, L.; Huang, J.; Pu, K.; James, T. D. Dual-Locked Spectroscopic Probes for Sensing and Therapy. *Nat. Rev. Chem.* **2021**, *5* (6), 406−421.
(59) Peng, H.; Wang, T.; Li, G.; Huang, J.; Yuan, Q. Dual-Locked Near-Infrared Fluorescent Probes for Precise Detection of Melanoma via Hydrogen Peroxide-Tyrosinase Cascade Activation. *Anal. Chem.* **2022**, *94* (2), 1070−1075.
(60) Almammadov, T.; Dirak, M.; Saymaz, A.; Acari, A.; Kolemen, S. A Hydrogen Sulfide and Tyrosinase Responsive Dual-Locked Fluorophore for Selective Imaging of Melanoma Cells. *Chem. Commun.* **2023**, *59* (66), 9972−9975.
(61) Westmeyer, G. G.; Emer, Y.; Lintelmann, J.; Jasanoff, A. MRI-Based Detection of Alkaline Phosphatase Gene Reporter Activity Using a Porphyrin Solubility Switch. *Cell Chem. Biol.* **2014**, *21* (3), 422−429.
(62) Haedicke, I. E.; Li, T.; Zhu, Y. L. K.; Martinez, F.; Hamilton, A. M.; Murrell, D. H.; Nofiele, J. T.; Cheng, H.-L. M.; Scholl, T. J.; Foster, P. J.; Zhang, X. An Enzyme-Activatable and Cell-Permeable Mn^{III}-Porphyrin as a Highly Efficient T_1 MRI Contrast Agent for Cell Labeling. *Chem. Sci.* **2016**, *7* (7), 4308−4317.
(63) Walter, E. R. H.; Ge, Y.; Mason, J. C.; Boyle, J. J.; Long, N. J. A Coumarin-Porphyrin FRET Break-Apart Probe for Heme Oxygenase-1. *J. Am. Chem. Soc.* **2021**, *143* (17), 6460−6469.
(64) Walsh, C.; Rajora, M. A.; Ding, L.; Nakamura, S.; Endisha, H.; Rockel, J.; Chen, J.; Kapoor, M.; Zheng, G. Protease-Activatable Porphyrin Molecular Beacon for Osteoarthritis Management. *Chem. Biomed. Imaging* **2023**, *1* (1), 66−80.
(65) Hirakawa, K.; Onishi, Y.; Ouyang, D.; Horiuchi, H.; Okazaki, S. PH-Dependent Photodynamic Activity of Bis(6-Methyl-3-Pyridylmethoxy)P(V)Tetrakis(P-Methoxyphenyl)Porphyrin. *Chem. Phys. Lett.* **2020**, *746*, 137315.
(66) Horiuchi, H.; Kuribara, R.; Hirabara, A.; Okutsu, T. PH-Response Optimization of Amino-Substituted Tetraphenylporphyrin Derivatives as PH-Activatable Photosensitizers. *J. Phys. Chem. A* **2016**, *120* (28), 5554−5561.
(67) Horiuchi, H.; Tajima, K.; Okutsu, T. Triply PH-Activatable Porphyrin as a Candidate Photosensitizer for Near-Infrared Photodynamic Therapy and Diagnosis. *J. Photochem. Photobiol. A* **2020**, *403*, 112846.
(68) Horiuchi, H.; Isogai, M.; Hirakawa, K.; Okutsu, T. Improvement of the ON/off Switching Performance of a PH-Activatable Porphyrin Derivative by the Introduction of Phosphorus(V). *ChemPhotoChem.* **2019**, *3* (3), 138−144.
(69) Chen, G.; Tang, M.; Fu, X.; Cheng, F.; Zou, X.; Wang, J.; Zeng, R. A Highly Sensitive and Selective Fluorescent Sensor for Detection of Sulfide Anion Based on the Steric Hindrance Effect. *J. Mol. Struct.* **2018**, *1151*, 230−235.
(70) Cheng, F.; Wu, X.; Liu, M.; Lon, Y.; Chen, G.; Zeng, R. A Porphyrin-Based Near-Infrared Fluorescent Sensor for Sulfur Ion Detection and Its Application in Living Cells. *Sensors and Actuators B Chemical* **2016**, *228*, 673−678.
(71) Liu, X.; Zhan, W.; Gao, G.; Jiang, Q.; Zhang, X.; Zhang, H.; Sun, X.; Han, W.; Wu, F.-G.; Liang, G. Apoptosis-Amplified Assembly of Porphyrin Nanofiber Enhances Photodynamic Therapy of Oral Tumor. *J. Am. Chem. Soc.* **2023**, *145* (14), 7918−7930.
(72) Lovell, J. F.; Jin, C. S.; Huynh, E.; Jin, H.; Kim, C.; Rubinstein, J. L.; Chan, W. C. W.; Cao, W.; Wang, L. V.; Zheng, G. Porphysome Nanovesicles Generated by Porphyrin Bilayers for Use as Multimodal Biophotonic Contrast Agents. *Nat. Mater.* **2011**, *10* (4), 324−332.
(73) Jin, C. S.; Cui, L.; Wang, F.; Chen, J.; Zheng, G. Targeting-Triggered Porphysome Nanostructure Disruption for Activatable Photodynamic Therapy. *Adv. Healthcare Mater.* **2014**, *3* (8), 1240−1249.
(74) Bandyopadhyay, S.; Zhao, Z.; East, A. K.; Hernandez, R. T.; Forzano, J. A.; Shapiro, B. A.; Yadav, A. K.; Swartchick, C. B.; Chan, J. Activity-Based Nitric Oxide-Responsive Porphyrin for Site-Selective and Nascent Cancer Ablation. *ACS Appl. Mater. Interfaces* **2024**, *16* (8), 9680−9689.
(75) Li, F.; Chen, C.; Yang, X.; He, X.; Zhao, Z.; Li, J.; Yu, Y.; Yang, X.; Wang, J. Acetal-Linked Hyperbranched Polyphosphoester Nanocarriers Loaded with Chlorin E6 for PH-Activatable Photodynamic Therapy. *ACS Appl. Mater. Interfaces* **2018**, *10* (25), 21198−21205.
(76) Zhu, X.; Lu, W.; Zhang, Y.; Reed, A.; Newton, B.; Fan, Z.; Yu, H.; Ray, P. C.; Gao, R. Imidazole-Modified Porphyrin as a PH-Responsive Sensitizer for Cancer Photodynamic Therapy. *Chem. Commun.* **2011**, *47* (37), 10311.
(77) Tian, J.; Ding, L.; Xu, H.-J.; Shen, Z.; Ju, H.; Jia, L.; Bao, L.; Yu, J.-S. Cell-Specific and PH-Activatable Rubyrin-Loaded Nanoparticles for Highly Selective Near-Infrared Photodynamic Therapy against Cancer. *J. Am. Chem. Soc.* **2013**, *135* (50), 18850−18858.
(78) Li, X.-S.; Ke, M.-R.; Huang, W.; Ye, C.-H.; Huang, J.-D. A PH-Responsive Layered Double Hydroxide (LDH)-Phthalocyanine Nanohybrid for Efficient Photodynamic Therapy. *Chem.—Eur. J.* **2015**, *21* (8), 3310−3317.
(79) Li, W.; Gandra, N.; Ellis, E. D.; Courtney, S.; Li, S.; Butler, E.; Gao, R. PH-Responsive, TiO_2-Attached Porphyrin for Singlet Oxygen Production in an Aqueous Solution. *ACS Appl. Mater. Interfaces* **2009**, *1* (8), 1778−1784.
(80) Li, F.; Chen, C.; Yang, X.; He, X.; Zhao, Z.; Li, J.; Yu, Y.; Yang, X.; Wang, J. Acetal-Linked Hyperbranched Polyphosphoester Nanocarriers Loaded with Chlorin E6 for PH-Activatable Photodynamic Therapy. *ACS Appl. Mater. Interfaces* **2018**, *10* (25), 21198−21205.
(81) Sun, B.; Chang, R.; Cao, S.; Yuan, C.; Zhao, L.; Yang, H.; Li, J.; Yan, X.; van Hest, J. C. M. Acid-Activatable Transmorphic Peptide-Based Nanomaterials for Photodynamic Therapy. *Angew. Chem., Int. Ed.* **2020**, *59* (46), 20582−20588.
(82) Ma, Y.; Li, X.; Li, A.; Yang, P.; Zhang, C.; Tang, B. H_2S-Activable MOF Nanoparticle Photosensitizer for Effective Photodynamic Therapy against Cancer with Controllable Singlet-Oxygen Release. *Angew. Chem.* **2017**, *129* (44), 13940−13944.
(83) Liu, F.; Ma, Y.; Xu, L.; Liu, L.; Zhang, W. Redox-Responsive Supramolecular Amphiphiles Constructed via Host-Guest Interactions for Photodynamic Therapy. *Biomater. Sci.* **2015**, *3* (8), 1218−1227.
(84) Xu, L.; Liu, L.; Liu, F.; Li, W.; Chen, R.; Gao, Y.; Zhang, W. Photodynamic Therapy of Oligoethylene Glycol Dendronized Reduction-Sensitive Porphyrins. *J. Mater. Chem. B* **2015**, *3* (15), 3062−3071.
(85) Cui, T.; Zhang, Y.; Qin, G.; Wei, Y.; Yang, J.; Huang, Y.; Ren, J.; Qu, X. A Neutrophil Mimicking Metal-Porphyrin-Based Nanodevice Loaded with Porcine Pancreatic Elastase for Cancer Therapy. *Nat. Commun.* **2023**, *14* (1), 1974.
(86) Pasparakis, G.; Manouras, T.; Vamvakaki, M.; Argitis, P. Harnessing Photochemical Internalization with Dual Degradable Nanoparticles for Combinatorial Photo-Chemotherapy. *Nat. Commun.* **2014**, *5* (1), 3623.
(87) Li, X.; Schumann, C.; Albarqi, H. A.; Lee, C. J.; Alani, A. W. G.; Bracha, S.; Milovancev, M.; Taratula, O.; Taratula, O. A Tumor-Activatable Theranostic Nanomedicine Platform for NIR Fluorescence-Guided Surgery and Combinatorial Phototherapy. *Theranostics* **2018**, *8* (3), 767−784.
(88) Lin, T.-Y.; Guo, W.; Long, Q.; Ma, A.-H.; Liu, Q.; Zhang, H.; Huang, Y.; Chandrasekaran, S.; Pan, C.-X.; Lam, K. S.; Li, Y. HSP90 Inhibitor Encapsulated Photo-Theranostic Nanoparticles for Syner-

https://doi.org/10.1021/jacsau.4c01108
JACS Au 2025, 5, 42−54

gistic Combination Cancer Therapy. *Theranostics* **2016**, *6* (9), 1324−1335.
(89) Chen, J.; Tan, X.; Huang, Y.; Xu, C.; Zeng, Z.; Shan, T.; Guan, Z.; Xu, X.; Huang, Z.; Zhao, C. Reactive Oxygen Species-Activated Self-Amplifying Prodrug Nanoagent for Tumor-Specific Cu-Chelate Chemotherapy and Cascaded Photodynamic Therapy. *Biomaterials* **2022**, *284*, 121513.
(90) Wang, Z.; Wang, N.; Cheng, S.-C.; Xu, K.; Deng, Z.; Chen, S.; Xu, Z.; Xie, K.; Tse, M.-K.; Shi, P.; Hirao, H.; Ko, C.-C.; Zhu, G. Phorbiplatin, a Highly Potent Pt(IV) Antitumor Prodrug That Can Be Controllably Activated by Red Light. *Chem.* **2019**, *5* (12), 3151−3165.
(91) Qiu, W.-X.; Liu, L.-H.; Li, S.-Y.; Lei, Q.; Luo, G.-F.; Zhang, X.-Z. ACPI Conjugated Gold Nanorods as Nanoplatform for Dual Image Guided Activatable Photodynamic and Photothermal Combined Therapy in Vivo. *Small* **2017**, *13* (18), 1603956.
(92) Wang, C.; Liu, L.; Cao, H.; Zhang, W. Intracellular GSH-Activated Galactoside Photosensitizers for Targeted Photodynamic Therapy and Chemotherapy. *Biomater. Sci.* **2017**, *5* (2), 274−284.
(93) Duan, X.; Zhang, G.; Ji, S.; Zhang, Y.; Li, J.; Ou, H.; Gao, Z.; Feng, G.; Ding, D. Activatable Persistent Luminescence from Porphyrin Derivatives and Supramolecular Probes with Imaging-Modality Transformable Characteristics for Improved Biological Applications. *Angew. Chem., Int. Ed.* **2022**, *61* (24), e202116174.
(94) Yang, L.; Zhao, M.; Chen, W.; Zhu, J.; Xu, W.; Li, Q.; Pu, K.; Miao, Q. A Highly Bright Near-Infrared Afterglow Luminophore for Activatable Ultrasensitive in Vivo Imaging. *Angew. Chem., Int. Ed.* **2024**, *63* (4), e202313117.
(95) Song, H.; Cai, Z.; Li, J.; Xiao, H.; Qi, R.; Zheng, M. Light Triggered Release of a Triple Action Porphyrin-Cisplatin Conjugate Evokes Stronger Immunogenic Cell Death for Chemotherapy, Photodynamic Therapy and Cancer Immunotherapy. *J. Nanobiotechnol.* **2022**, *20* (1), 329.
(96) Tang, M.; Song, Y.; Lu, Y.-L.; Zhang, Y.-M.; Yu, Z.; Xu, X.; Liu, Y. Cyclodextrin-Activated Porphyrin Photosensitization for Boosting Self-Cleavable Drug Release. *J. Med. Chem.* **2022**, *65* (9), 6764−6774.
(97) Ma, X.; Wang, P.; Wu, Q.; Zhou, J.; Wang, D.; Yadav, D.; Zhang, H.; Zhang, Y. Porphyrin Centered Paclitaxel Tetrameric Prodrug Nanoassemblies as Tumor-Selective Theranostics for Synergized Breast Cancer Therapy. *Adv. Healthcare Mater.* **2023**, *12* (2), 2202024.
(98) Kawasaki, R.; Yamana, K.; Shimada, R.; Sugikawa, K.; Ikeda, A. Water Solubilization and Thermal Stimuli-Triggered Release of Porphyrin Derivatives Using Thermoresponsive Polysaccharide Hydroxypropyl Cellulose for Mitochondria-Targeted Photodynamic Therapy. *ACS Omega* **2021**, *6* (4), 3209−3217.
(99) Pei, P.; Sun, C.; Tao, W.; Li, J.; Yang, X.; Wang, J. ROS-Sensitive Thioketal-Linked Polyphosphoester-Doxorubicin Conjugate for Precise Phototriggered Locoregional Chemotherapy. *Biomaterials* **2019**, *188*, 74−82.
(100) Sekhar, A. R.; Chitose, Y.; Janoš, J.; Dangoor, S. I.; Ramundo, A.; Satchi-Fainaro, R.; Slavíček, P.; Klán, P.; Weinstain, R. Porphyrin as a Versatile Visible-Light-Activatable Organic/Metal Hybrid Photoremovable Protecting Group. *Nat. Commun.* **2022**, *13* (1), 3614.
(101) Deng, C.; Zheng, M.; Han, S.; Wang, Y.; Xin, J.; Aras, O.; Cheng, L.; An, F. GSH-Activated Porphyrin Sonosensitizer Prodrug for Fluorescence Imaging-Guided Cancer Sonodynamic Therapy. *Adv. Funct. Mater.* **2023**, *33* (32), 2300348.
(102) Hu, H.; Wang, H.; Yang, Y.; Xu, J.; Zhang, X. A Bacteria-Responsive Porphyrin for Adaptable Photodynamic/Photothermal Therapy. *Angew. Chem., Int. Ed.* **2022**, *61* (23), e202200799.

https://doi.org/10.1021/jacsau.4c01108
JACS Au 2025, 5, 42−54